JOURNAL OF MATERIALS SCIENCE 30(1995) 3561–3566

Effects of microstructures on the cyclic deformation behaviour of SiC_w/Al composite

D. Z. WANG, J. LIU, C. K. YAO
Department of Metals and Technology, Harbin Institute of Technology, Harbin, 150006 People's Republic of China

W. C. YU, Z. G. WANG
State Key Laboratory for Fatigue and Failure of Materials, Institute of Metal Research, Academia Sinica, Shenyang, 110015 People's Republic of China

The cyclic deformation behaviour of an aluminium matrix composite reinforced with 16% V_f silicon carbide whiskers was studied. The microstructures were designed so that different precipitates existed in the composite. The results indicated that the SiC_w/6061 Al composite demonstrated cyclic hardening, however the cyclic response stresses and the cyclic hardening tendency were different under differing ageing conditions. Lower cyclic response stresses and higher hardening tendencies were found under natural ageing conditions, while higher cyclic response stresses and lower hardening tendencies were obtained under artificial ageing conditions. The higher the cyclic response stresses following artificial ageing, the lower the hardening tendencies that reduced fatigue life. The effects of microstructures on the cyclic deformation behaviour of the composite were examined under the TEM and changes in microstructure caused by the cyclic deformation were observed.

1. Introduction

Silicon carbide whisker reinforced aluminium alloy composites (SiC_w/Al) are especially attractive in aeronautic and astronautic industries because of their high specific strength and modulus, thermostability, promising high temperature properties, good wear resistance, and may be used in the near future [1–4]. Since fatigue has generally turned out to be the most frequent cause of service failure, great emphasis has been placed on this subject during the past ten years [5–10]. However, most of these reports were on the high cycle fatigue properties and the initiation and propagation behaviour of fatigue cracks and only limited data is available on the cyclic deformation behaviour of the composite. Williams *et al.* [6] found that 20% V_f–SiC_w/ 2124 Al–T6 show cyclic hardening, and exhibited higher cyclic yield strength compared to the unreinforced 2124 Al alloy.

The changes caused by the cyclic deformation were similar in both the composite and the unreinforced alloy: elastic modulus remained almost unchanged, yield strength increased for about 16% and the compressive cyclic yield strength was slightly higher than the tensile cyclic yield strength. It was thought by the authors [6] that the cyclic hardening in the composite was the result of increased dislocation movement resistance caused by the whiskers. As the cyclic deformation behaviour is very sensitive to the microstructure, it is quite necessary to study the effects of microstructure, such as precipitates and whiskers, on the cyclic deformation behaviour of SiC_w/Al composite. Therefore, the present work was carried out to study the cyclic deformation behaviour of a SiC_w/6061 Al composite, especially with the emphasis on the effects of microstructure.

2. Experimental procedure

The composite used in this study was 6061 aluminium alloy reinforced with 16% V_f silicon carbide whisker, processed using the squeeze casting method and provided by the Institute of MMC Research, Harbin Institute of Technology (HIT). An unreinforced 6061 Al alloy was used as a control alloy for comparison.

The SiC whiskers were provided by Tokai Carbon Co., Japan. The average dimensions of the whiskers were $0.3 \sim 0.6\,\mu m$ in diameter and $10 \sim 40\,\mu m$ in length before processing. Due to the breakage during processing, the average whisker length was reduced to $2 \sim 5\,\mu m$.

The squeeze-cast billets of the composite were hot extruded into two plates of dimension $5 \times 30 \times 300$ mm at 420 °C. Then the plates were solutionized at 520 °C for one hour. In order to investigate the effects of matrix precipitates on the cyclic deformation behaviour of the composite, different ageing conditions were selected: 150 °C for 10 hours, 170 °C for 15 hours and natural ageing for 50 days.

After the heat treatment, dog-bone-shaped specimens with the work region of $2.5 \sim 3 \times 5 \times 12$ mm were cut out along the extrusion direction. The surfaces of all specimens were mechanically polished carefully. Cyclic deformation tests were carried out on a 10 kN Schenck servohydraulic system at the strain

0022–2461

rate of 0.002 ~ 0.004 s^{-1} and strain ratio of -1 under strain control. Thin foils for TEM observations from the free surfaces of the fatigued specimens were made by ion thinning method. Thin foils for TEM examination of the precipitates were prepared by electropolishing in 70 ml:30 ml methanol:nitric acid using 15 V and 30 mA at $-20\,^{\circ}C$ in order to minimize the effects of specimen preparation on the results. Microstructures of the composite before and after cyclic deformation were examined on a Philips EM420 TEM at 100 kV.

3. Experimental results

3.1. Cyclic deformation behaviour

Fig. 1 shows the variation of the stress amplitude against the number of cycles for the composite and the unreinforced 6061 Al alloy in naturally aged condition. It can be seen that both the reinforced and control 6061 Al show cyclic hardening. However the hardening tendencies are slightly different. The composite shows cyclic hardening immediately after the cyclic load is applied and the larger the applied strain amplitude, the higher is the hardening tendency. The control 6061 Al alloy shows an increased hardening rate only after a few cycles of load are applied. This result suggests that the work hardening rate is higher in the composite.

Fig. 2 shows the cyclic deformation response of the composite and the control 6061 Al alloy in artificial ageing conditions. As compared to that in Fig. 1, the initial cyclic response stresses are increased while the hardening tendencies decreased. It can also be seen in Fig. 2 that both the composite and the control 6061 Al alloy show hardly any hardening until the applied strain amplitude is larger than 0.005.

The cyclic strain amplitude versus number of cycles to failure for the composite and the matrix alloy after nature ageing and artificial ageing is shown in Fig. 3. The control 6061 Al in natural aged condition exhibits the longest low cycle fatigue life and the composite under 170 °C ageing condition the shortest for the same loading condition. The above results indicate that the composite has no advantages over the control 6061 Al alloy in low cycle fatigue, especially for the composite in the harder state.

3.2. Microstructure before cyclic deformation

Microstructures of the SiC_w/6061 Al composite and the unreinforced 6061 Al alloy before cyclic deformation are shown in Figs 4–6. High density dislocations are found in the composite (Fig. 4a). These dislocations are usually pinned by SiC whiskers and form forest dislocations, which will impede the movement of other dislocations. Fig. 4b shows the dislocations in the unreinforced 6061 Al alloy. The dislocation density is quite low, and they are impeded by inclusions.

The micrograph of Fig. 5 shows the matrix grain in the composite. There are always one to two grains between two groups of parallel SiC whiskers, and the size of the grains is one to two micrometres.

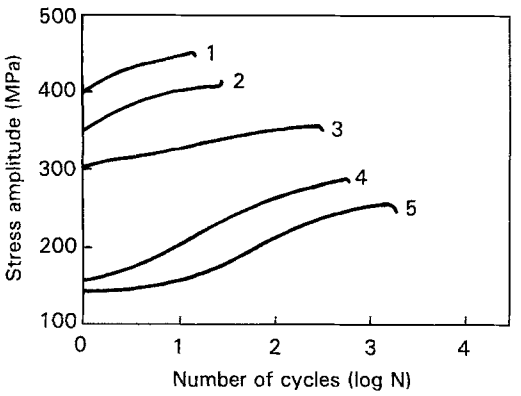

Figure 1 Stress amplitude versus number of cycles of SiC_w/6061Al and 6061Al natural-aged for 50 days: (1) – SiC_w/6061Al $\Delta\varepsilon t/2 = 0.0095$; (2) – SiC_w/6061Al $\Delta\varepsilon t/2 = 0.0076$; (3) – SiC_w/6061Al $\Delta\varepsilon t/2 = 0.0056$; (4) – 6061Al $\Delta\varepsilon t/2 = 0.0097$; (5) – 6061Al $\Delta\varepsilon t/2 = 0.0058$.

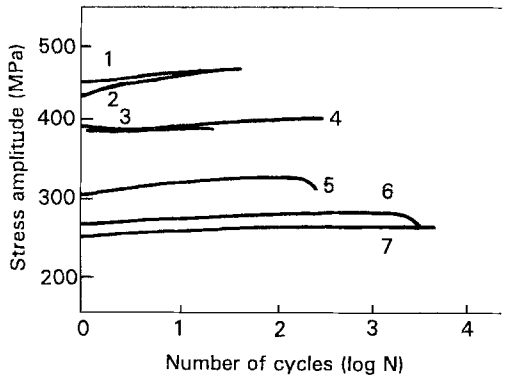

Figure 2 Stress amplitude versus number of cycles for SiC_w/6061Al and 6061Al in artificial aged condition: (1) – SiC_w/6061Al 170 °C for 15 hrs $\Delta\varepsilon t/2 = 0.0076$; (2) – SiC_w/6061Al 150 °C for 10 hrs $\Delta\varepsilon t/2 = 0.0076$; (3) – SiC_w/6061Al 170 °C for 15 hrs $\Delta\varepsilon t/2 = 0.0055$; (4) – SiC_w/6061Al 150 °C for 10 hrs $\Delta\varepsilon t/2 = 0.0055$; (5) – 6061Al 150 °C for 12 hrs $\Delta\varepsilon t/2 = 0.0077$; (6) – 6061Al 150 °C for 12 hrs $\Delta\varepsilon t/2 = 0.0055$; (7) – 6061Al 150 °C for 12 hrs $\Delta\varepsilon t/2 = 0.0043$.

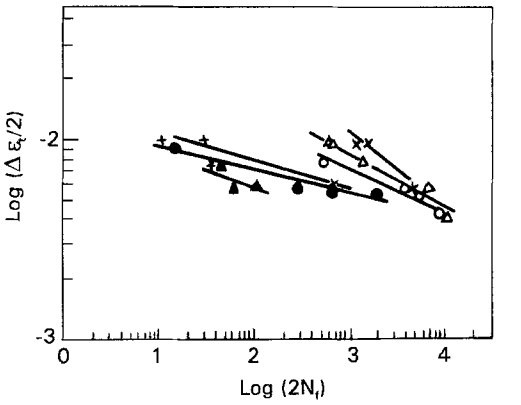

Figure 3 Strain amplitude versus number of cycles to failure for SiC_w/6061Al and 6061Al; (×) 6061Al, natural aged for 50 days; (Δ) 6061Al, 150 °C ageing for 12 hrs; (○) 6061Al, 170 °C ageing for 15 hrs; (+) SiC_w/6061Al, natural aged for 50 days; (●) SiC_w/6061Al, 150 °C ageing for 10 hrs; (▲) SiC_w/6061Al, 170 °C ageing for 15 hrs.

Fig. 6 shows the precipitates in the reinforced and control 6061 Al alloy. The needle-shaped precipitates formed in the control 6061 Al alloy after 75 hours ageing at 170 °C are shown in Fig. 6a. It can be seen

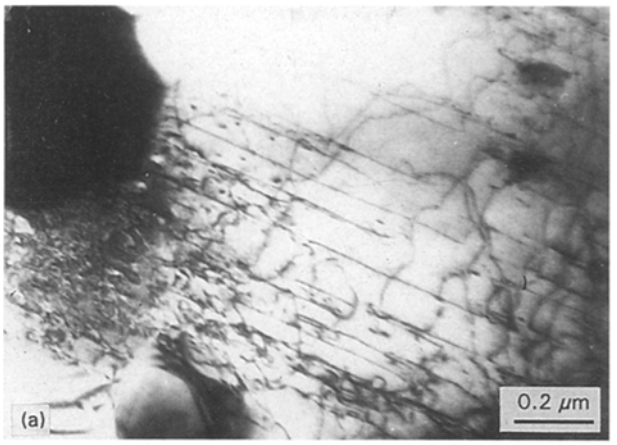

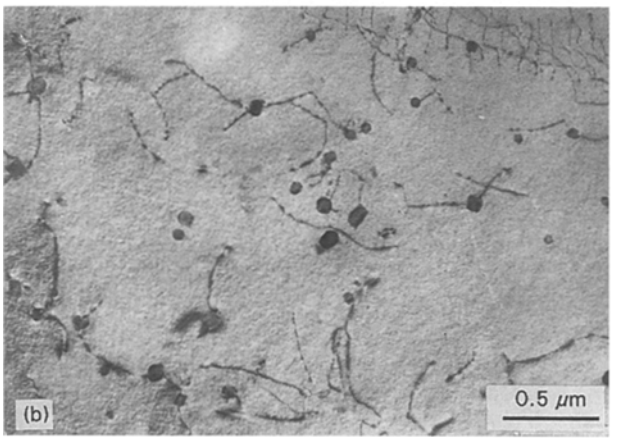

Figure 4 Dislocations in SiC_w/6061Al and 6061Al before cyclic deformation; (a) SiC_w/6061Al; (b) 6061.

that these precipitates grow on the {0 0 1} plates along the ⟨1 0 0⟩ directions of the matrix. The diffraction pattern is characteristic of GP zones in the Al–Mg–Si alloy [11]. And hence, it can be considered that the needle shaped precipitates are GP zones. The precipitates in the composite after 150 °C/10 hours ageing and 170 °C/15 hours ageing are shown in Fig. 6b and 6c respectively, in which spherical (Fig. 6b) and needle-shaped (Fig. 6c) GP zones are found. The TEM observation demonstrates that the GP zones are uniformly distributed in the matrix alloy, and no precipitate-free zone or preferential precipitation at or near the SiC–Al interface are found. No distinct precipitate is found in the naturally aged composite.

3.3. Dislocation structure after cyclic deformation

Microstructures in the composite after cyclic deformation are shown in Figs 7–11.

Fig. 7 demonstrates that dislocation density is increased after the cyclic deformation in the naturally aged composite, especially when the applied strain amplitude is large. And the pattern of dislocation changes from "lines" to "tangles".

Fig. 8 shows the microstructure after cyclic deformation in the 150 °C/10 hours aged composite. When the total strain amplitude is small (0.0054), the linear

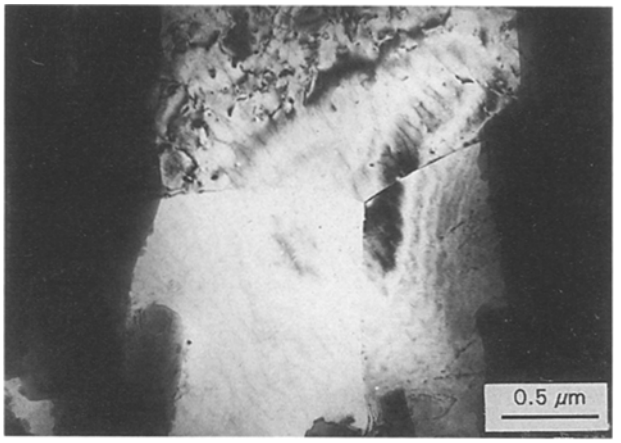

Figure 5 Matrix grains in SiC_w/6061Al.

character of dislocation still exists, although a few loops and tangles can also be found (Fig. 8a). When the total strain amplitude is large (0.0076), dislocation lines disappear, and loops as well as dislocation tangles appear (Fig. 8b). Also, the density of dislocation is higher in Fig. 8b than that in Fig. 8a. By using the weak beam dark field imagine technique, it can be seen that the dislocations bow out and leave dislocation loops around the spherical GP zones when they by-pass the precipitates (Fig. 8c). Although the average distance between the spherical GP zones is not more than 10 nm, the space in which the dislocation line can bow out is about 100 nm.

Fig. 9, which is a micrograph of interaction of dislocations with precipitates in the 170 °C/15 hours aged composite, shows that the space in which dislocations can bow out is smaller than that in the 150 °C/10 hours aged composite. This suggests that the needle-shaped GP zones are more effective in impeding the movement of dislocations.

Fig. 10 shows the different dislocation characteristics after the cyclic deformation in the matrix of the composite at the end and the lateral surface of an SiC whisker after the 170 °C/15 hours ageing. An important feature of this is that the dislocation density in the matrix grain is higher at the whisker end (Fig. 10a) than at the lateral surface (Fig. 10b), also, dislocation tangles are found in the matrix grain at the whisker end.

Fig. 11 shows the effects of matrix grain boundary on the movement of dislocation in the composite. The thin foil is obtained from the 150 °C/10 hours aged composite which is cyclic deformed with a total strain amplitude of 0.0064. It can be seen that matrix grain boundary can also act as an obstacle to the movement of dislocations.

4. Discussion

4.1. Effects of ageing condition on the cyclic deformation behaviour of SiC_w/6061 Al composite

The obvious differences in the cyclic deformation responses and low cycle fatigue life between the

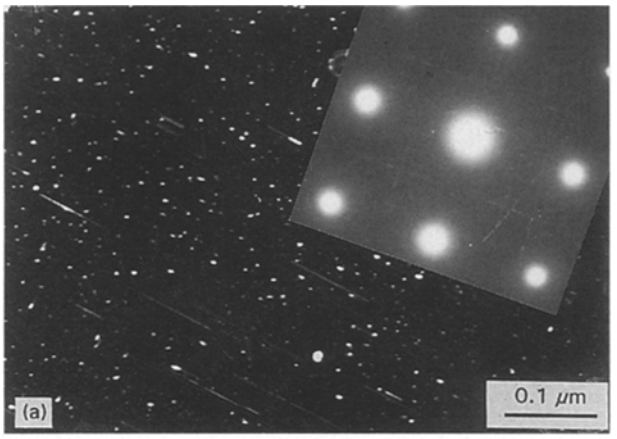

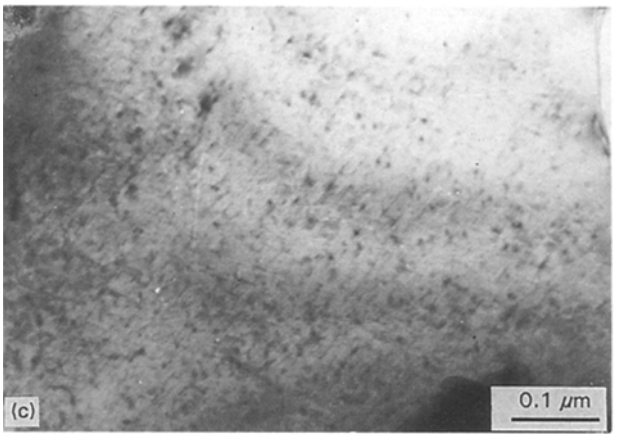

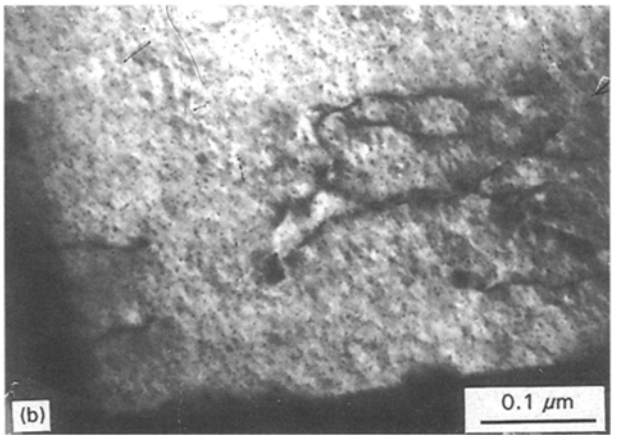

Figure 6 Precipitates in SiC_w/6061Al and 6061Al after artificial ageing; (a). in 6061Al after 75 hrs ageing at 170 °C; (b) in SiC_w/6061Al after 10 hrs ageing at 150 °C; (c) in SiC_w/6061Al after 15 hrs ageing at 170 °C.

SiC_w/6061 Al composite and the control 6061 Al alloy in different ageing conditions indicate that ageing conditions have a greater effect on the cyclic deformation behaviour of the composite.

In aluminium alloys it is generally agreed that the effects of precipitates on the cyclic deformation behaviour are determined by their structure and properties. When the precipitates are shearable, some of them will be cut by dislocations moving on the slip planes, and the ultimate disappearance of these precipitates will result in cyclic softening. However, when the precipitates are unshearable, they will impede the movement of dislocations, and the dislocations have to bow out or climb to by-pass the precipitates. The result of the increase of dislocation density is that the alloys show cyclic hardening.

The results of the present work indicate that the cyclic hardening of the composite is also caused by the increase of dislocation density. Hence the cyclic response stress and the cyclic hardening tendency can be affected by ageing conditions. When no precipitate exists in the composite, the main obstacles to the movement of dislocations are SiC whiskers, forest dislocations and matrix grain boundaries, and the mobility of dislocations is relatively large, so the composite exhibits lower cyclic response stresses and higher cyclic hardening tendency than that in the artificially aged composite. When spherical or needle-shaped precipitates exist in the composite, however, the movement of dislocations is impeded not only by the obstacles stated above, but also by these precipitates, and hence, the decrease in mobility of dislocations leads to a higher cyclic response stresses and lower hardening tendency, especially for the composite containing needle-shaped GP zones which can impede the movement of dislocations more effectively.

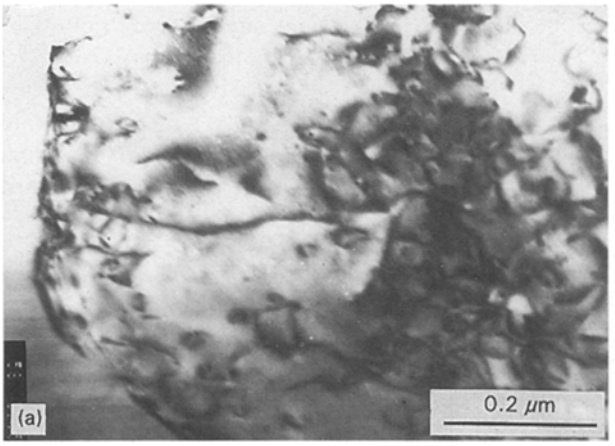

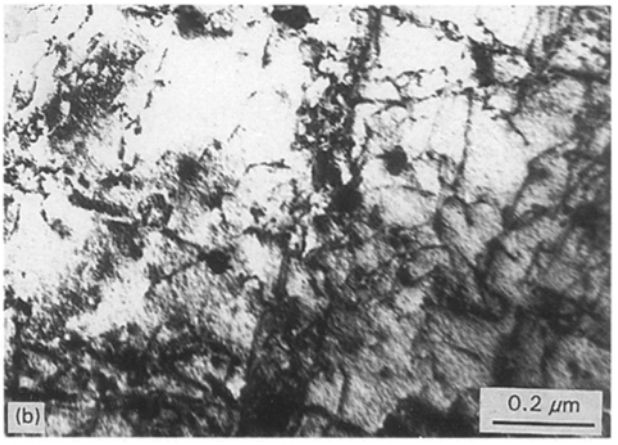

Figure 7 Dislocations in naturally aged SiC_w/6061Al after cyclic deformation; (a) $\Delta\varepsilon t/2 = 0.0057$; (b) $\Delta\varepsilon t/2 = 0.0095$.

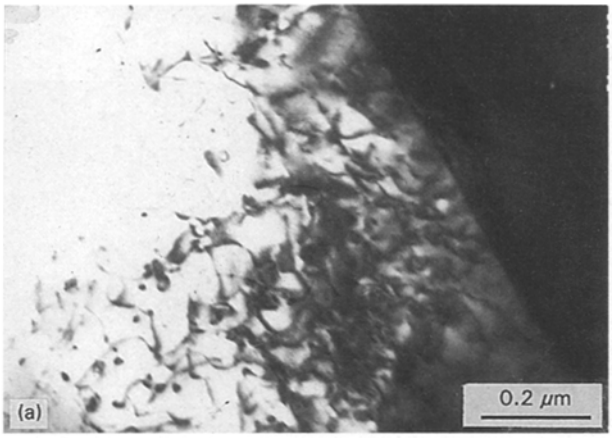

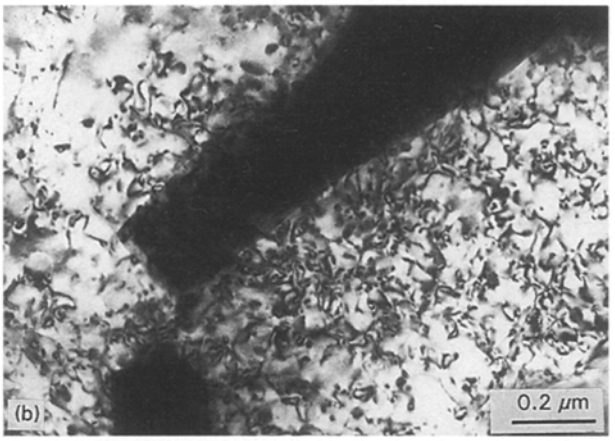

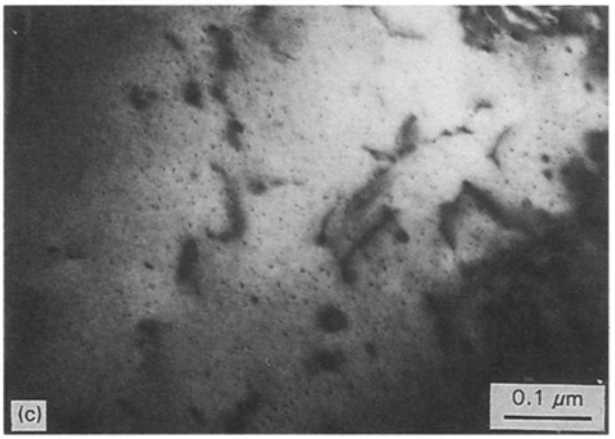

Figure 8 Dislocations in 150 °C aged SiC_w/6061Al after cyclic deformation: (a) $\Delta\varepsilon t/2 = 0.0054$; (b) $\Delta\varepsilon t/2 = 0.0076$; (c) $\Delta\varepsilon t/2 = 0.0076$.

4.2. Effects of SiC whiskers on the cyclic deformation behaviour of SiC_w/6061 Al composite

The present experimental results on the cyclic deformation behaviour of naturally aged composite and the unreinforced 6061 Al alloy show that the cyclic response stresses are higher in the composite, although no distinct precipitates are found in either of them. This suggests that factors other than the precipitates must exist to affect the fatigued properties.

SiC whiskers are the most important components in the SiC_w/6061 Al composite, and they can affect the cyclic deformation behaviour of the composite in the following ways.

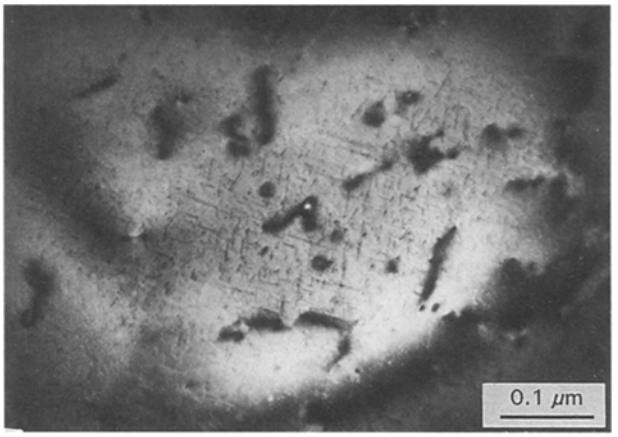

Figure 9 Interaction of dislocations with needle-shaped precipitates in 170 °C aged SiC_w/6061Al after cyclic deformation ($\Delta\varepsilon t/2 = 0.0057$).

SiC whiskers can restrain the deformation of the matrix directly. It is believed that the bonding of SiC_w–Al interface is strong enough [12] to transfer the load, so the whiskers can restrain the deformation of the matrix near them. The present study indicates that the restrained deformation mainly occurred at the lateral surfaces of whiskers when the applied load is parallel to the orientation of extrusion (Fig. 8a and Fig. 10). At the whisker ends, the restraint effect decreases, and furthermore, large stress concentration exists at whisker ends when the external load is applied [4]. Hence, severe matrix deformation still exists at whisker ends although the deformation of the matrix is restrained in the grains at the lateral surfaces of the whiskers.

SiC whiskers can affect the cyclic deformation behaviour of the composite indirectly by affecting the microstructure of the composite. The introduction of SiC whiskers to the aluminium alloy will result in a high density of dislocations in the Al–matrix because of the large ratio of thermal expansion coefficients (10:1) between Al and SiC [13]. These dislocations are usually pinned by SiC whiskers and form forest dislocations (Fig. 4a), which will act as obstacles to the movement of other dislocations. Furthermore, since the composite used in this study was made by squeeze casting method, the existence of SiC whiskers will restrain the growth of matrix grains during the process of solidification. The fine matrix grains will also prohibit the deformation of the matrix in the composite.

5. Conclusions

(i) SiC_w/6061 Al composite shows cyclic hardening in the conditions of natural and artificial ageing, which resulted from the increase of dislocation density caused by the cyclic deformation.

(ii) The high cyclic response stresses of SiC_w/6061 Al composite can be attributed to multiple factors, including the restrained deformation of the matrix caused by precipitates, SiC whiskers, forest dislocations and fine matrix grains.

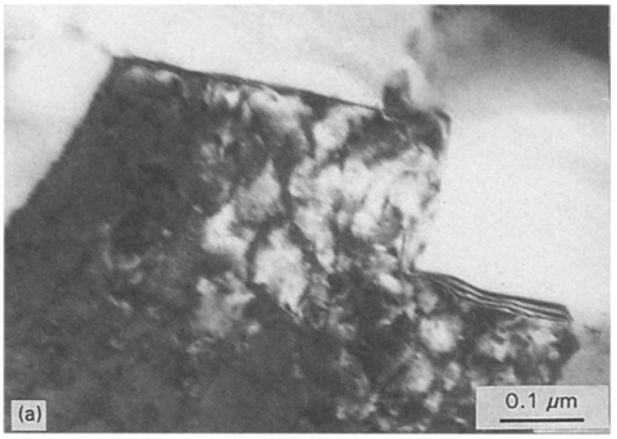

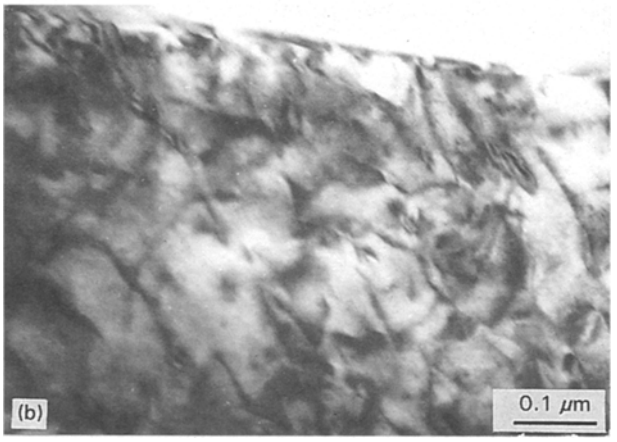

Figure 10 Dislocations in 170 °C aged SiC_w/6061Al after cyclic deformation ($\Delta\varepsilon t/2 = 0.0076$); (a) at SiC whisker end; (b) near SiC whisker lateral surface.

(iii) Ageing condition has a great effect on the cyclic deformation behaviour of SiC_w/6061 Al composite. The higher cyclic response stresses the composite has after the ageing treatment, the lower the cyclic hardening tendency and the lower the cycle fatigue life it exhibits.

(iv) SiC whiskers affect the cyclic deformation behaviour of the composite in two ways. First, they restrain the deformation of the matrix near their lateral surfaces, and promote the deformation of the matrix at their ends directly. Secondly, they introduce high density dislocations and refine the matrix grains in the composite which can also restrain the deformation of the matrix in the composite.

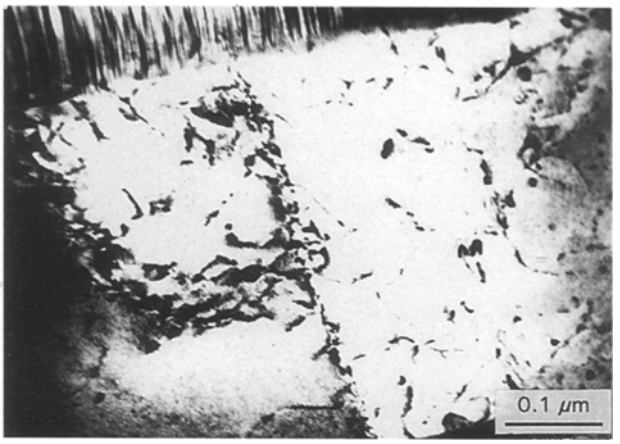

Figure 11 Effects of matrix grain boundary on the movement of dislocations in 150 °C aged SiC_w/6061Al.

References

1. R. J. LEDERICH and S. M. L. SASTRY, *Mater. Sci. Eng.* **2** (1982) 143.
2. W. R. MOHN and D. VUKOBRATOVICH, *SAMPE J.* **24** (1988) 26.
3. Z. Y. MA and C. K. YAO, *Mater. Chem. Phys.* **25** (1990) 463.
4. J. M. PAPAZIAN and P. N. ADLER, *Metall. Trans. A* **21A** (1990) 411.
5. C. R. CROWE and D. F. HASSON, Proceedings of Strength of Metals and Alloys, Melbourne, Australia (1982) p. 859.
6. D. R. WILLIAMS and M. E. FINE, Proceedings, of the 5th ICCM, USA (1985) 639.
7. W. A. LOGSDON and P. K. LIAW, *Eng. Fract. Mech.* **24** (1986) 737.
8. C. MASUDA and Y. TANAKA, *Tetsu-To-Hagane* **9** (1989) 339.
9. S. J. HARRIS and G. YI, Proceedings of the 7th ICCM, Guangzhou, People's Republic of China (1989) 659.
10. J. LIU, D. Z. WANG, C. K. YAO, W. C. YU and Z. G. WANG, *J. Mater. Sci. Lett.* **11** (1992) 970.
11. M. H. JACOBS, *Phil. Mag.* **26** (1972) 1.
12. P. K. LIAW, J. G. GREGGL and W. A. LOGSDON, *J. Mater. Sci.* **22** (1987) 1613.
13. M. VOGELSANG, R. J. ARSENAULT and R. M. FISHER, *Metall. Trans. A* **17A** (1986) 379.

Received 9 September 1993
accepted 6 July 1994